Airborne electromagnetic measurements of sea ice thickness: methods and applications

Christian Haas, Sibylle Goebell, Stefan Hendricks, Torge Martin, Andreas Pfaffling, Carola von Saldern, AWI

Abstract
Alfred Wegener Institute operates two helicopter-borne electromagnetic (EM) sounding devices dedicated to the measurement of sea ice thickness. With the method, level total (ice plus snow) thickness can be determined with an accuracy of ±0.1 m. However, due to the footprint of the method and due to the porosity of unconsolidated ridge keels, deformed ice thickness can be strongly underestimated. The paper summarizes the retrieval of ice thickness from the EM data, and shows some validation results. Applications of the methods show that level ice thickness has decreased by 20% in the Transpolar drift between 1991 and 2001, but remained constant at 2.0 m between 2001 and 2004. Surveys in 2004 and 2005 in the Lincoln Sea revealed very thick ice with modal thicknesses between 3.9 and 4.2 m, and an increase of mean ice thickness from 4.67 m in 2004 to 5.18 m in 2005. As the EM instruments also comprise a laser altimeter and a differential GPS receiver (DGPS), independent measurements of ridge distributions and surface roughness can be obtained. In addition, coincident measurements of total thickness and surface elevation allow the retrieval of snow thickness.

1. Introduction

Sea ice thickness is one of the most important parameters for climate studies and ice engineering problems. Apart from upward looking sonar (ULS) profiling, electromagnetic induction (EM) thickness sounding has become an accurate and efficient method for thickness profiling and can be operated on the ice, from ships (Haas, 1998; Haas et al., 1999), or from structures like lighthouses or oil rigs (Haas and Jochmann, 2003). However, EM sounding is most powerful when operated from helicopters (Kovacs et al., 1987; Kovacs and Holladay, 1990; Prinsenberg and Holladay 1993; Haas, 2004; Haas et al., 2006) or fixed-wing aircrafts (Multala et al., 1996).

At Alfred Wegener Institute for Polar and Marine Research in Bremerhaven, Germany, two helicopter EM (HEM) systems have been developed since 1999 (EM birds), based on good experience on the robustness and efficiency of EM thickness measurements in general (Haas et al., 1997; Haas and Eicken, 2001). Those two birds have since then been widely operated in Arctic, Antarctic, and Baltic Sea waters, providing unique new insights into regional ice thickness distributions and their temporal changes.

Here, we review the HEM method and discuss the accuracy of HEM thickness retrievals. Some of the most recent results are summarized. Then, a final section shows how HEM measurements can be applied for advanced studies of delineating ice regimes from surface or satellite remote sensing data, and for the determination of snow thickness if the thickness retrievals are combined with laser altimeter and GPS measurements. Most results were obtained within the EU-funded GreenICE (Greenlandic Arctic Shelf Ice and Climate Experiment) and SITHOS (Sea Ice Thickness Observing System) projects between 2003 and 2005.

2. Methods

2.1 HEM thickness sounding

An EM system consists of an assembly of coils for the transmission and reception of low-frequency EM fields, and a laser altimeter. The EM components are sensitive to the sensors height above the conductive sea water surface, while the sensors altitude above the ice or snow surface is determined with the laser altimeter. Over sea ice, the water surface coincides with the ice underside. Therefore, the difference of the height measurements of both components corresponds to the ice-plus-snow, or total thickness (Figure 1; Haas, 1998).

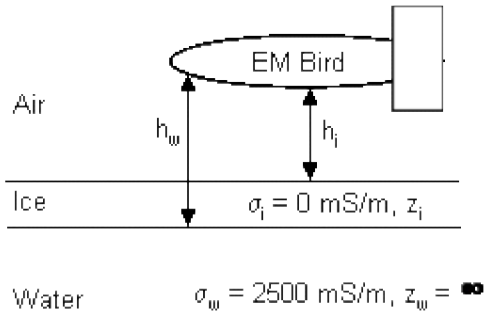

Figure 1: Principle of EM thickness sounding, using a bird with transmitter and receiver coils and a laser altimeter. Ice thickness z_i is obtained from the difference of measurements of the bird's height above the water and ice surface, h_w and h_s, respectively. H_w is obtained with the assumption of a negligible ice conductivity s_i, known water conductivity s_w, and horizontal layering (see below).

2.2 AWI EM birds

We have built two EM birds dedicated to scientific sea ice studies. This requires that they have to be easily operable from any kind of helicopter capable of carrying an external load, and from board icebreakers (Figure 2). Therefore, our birds are only 3.5 m long and weigh 100 kg. They are suspended 20 m below the helicopter and are towed at heights of 10 to 20 m above the ice surface. One two-frequency EM bird operates at frequencies of 3.6 and 112 kHz, and our single-frequency bird uses a signal frequency of 4.1 kHz. Coil spacing is 2.77 m for the low frequency transmitting and receiving coils, and 2.05 m for the high frequency. Signal generation, reception, and processing are fully digital, maximising signal-to-noise ratio. The EM systems are calibrated by means of internal calibration coils with a known response. EM sampling frequency is 10 Hz, corresponding to a measurement point spacing of approximately 3 to 4 m. Measurements are interrupted every 15 to 20 minutes by ascents to high altitude, to monitor electrical system drift.

Figure 2: AWI HEM bird during take-off from the helicopter deck of an icebreaker, and during operation at 15 to 20 m above the ice surface (right photo courtesy J. Wilkinson).

2.3 Thickness retrieval

For the thickness computation over high salinity sea water, we use only data of the in-phase component of the complex EM signal, which is the strongest and most sensitive channel. Figure 3 shows the relationship between bird height above the ice surface and the measured and modelled EM responses for a flight over the Lincoln Sea. The model results (Ward and Hohmann, 1988) have been computed for open water (ice thickness 0 m) with a sea water conductivity of 2500 mS/m, representative of in-situ CTD measurements. The model curve provides the general means of computing the height of the bird above the water surface or ice underside from a measurement of in-phase EM field strength at a certain height above the water (Figure 1; Haas, 1998). Measurements at different heights are obtained because the altitude of the helicopter and bird vary between 10 and 25 m during the flight (Figure 3). The data can be separated into two branches: while open water measurements at different bird heights agree well with the model curves, the presence of sea ice leads to a reduction of the measured EM signal at a given laser height (Fig. 3). Therefore the scattered cloud of data points below the model curve represents measurements over ice. Ice thickness is computed by subtracting the laser height measurement over sea ice from the model curve (Haas, 1998). It can also be visually estimated from the horizontal distance between each EM measurement and the model curve (Fig. 3). The thickness computation assumes a negligible sea ice conductivity of < 20 mS/m, which is likely for the multiyear ice in the study region (Haas et al., 1997).

Figure 4 illustrates the two steps of determining the height above the ice and water surfaces, and obtaining ice thickness from the difference of these measurements. The example is from the Transpolar Drift in August 2001. Figure 4c shows the thickness distribution computed from the resulting ice thickness profile, computed with a bin width of 0.1 m. The modes of the distribution represent the fraction of open water along the profile, first year ice with a modal thickness of 1.2 m, and 2 m thick second and multiyear ice. The narrowness of the modes demonstrates the low noise and high accuracy of our measurements, which we estimate to be better than ±0.1 m.

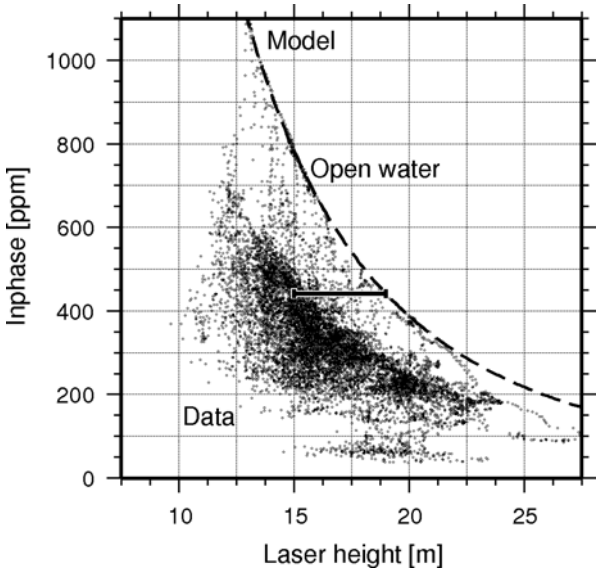

Figure 3: EM field strength (in-phase component of relative secondary field strength at 3.6 kHz) versus laser height measurement. A model curve and data over a typical ice surface with some leads are shown. The model curve has been computed for a sea water conductivity of 2500 mS/m. The horizontal bar illustrates how ice thickness (4 m) is obtained for a single data point from the difference between laser measurement and the model curve for a given EM field strength (see text).

2.4 Validation of EM thickness retrievals

Comparison with drill-hole data shows that the EM derived ice thicknesses agree well within ±0.1 m over level ice (e.g. Reid et al., 2006, Pfaffling et al., 2006; see also Fig. 8 below). Figure 5 shows an example of a 150 m long drill-hole profile compared to the HEM thickness retrievals. However, the accuracy is worse over ridges. Because the low-frequency EM field is diffusive, its strength represents the average thickness of an area of 3.7 times the instruments altitude above the ice surface (Kovacs et al., 1995; Reid et al., 2006). Due to this “footprint” and the porous nature of ridge keels, the maximum ridge thickness can be strongly underestimated. A study by Reid et al. (2006) shows that the footprint of the Quadrature component of the EM signal amounts only to half or two-thirds of the Inphase footprint. This can also be judged from Figure 5. However, we normally use the Inphase component because it has a much better signal-to-noise ratio.

Haas and Jochmann (2003) have performed coincident ULS and EM measurements on a lighthouse in the Bay of Bothnia of the Baltic Sea, allowing for a direct comparison of ULS draft and EM thickness measurements of deformed ice thickness. These showed that the thickness of unconsolidated deformed ice is underestimated by the EM measurements by as much as 50 or 60% in the worst cases, depending on the geometry and consolidation of the keels (Figure 6). It should be noted, however, that the example of Figure 6 has been obtained over brackish sea water where the measurements are hampered by low EM responses. Other experience shows that the performance of the EM measurements over consolidated ridges under Arctic conditions is much better (Figure 5).

a)

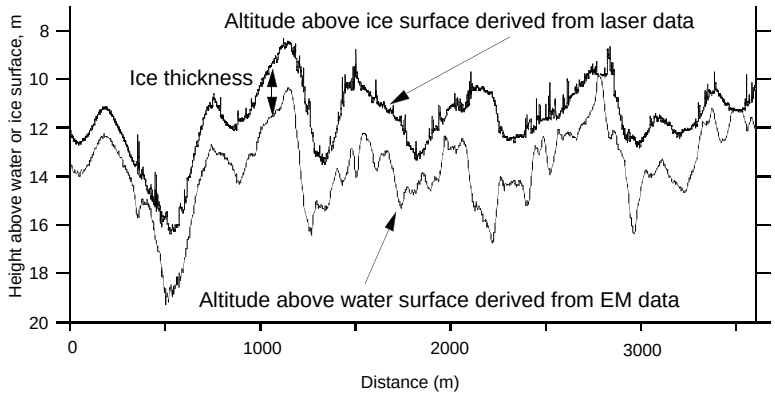

b)

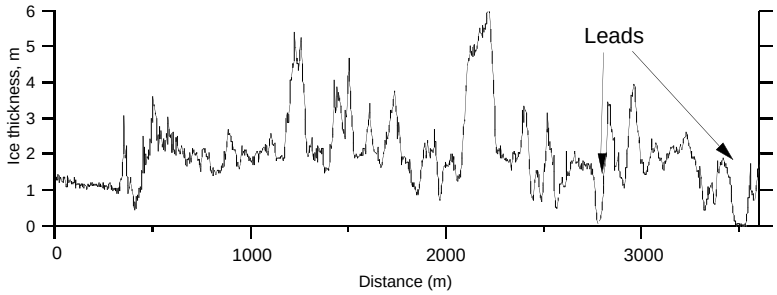

c)

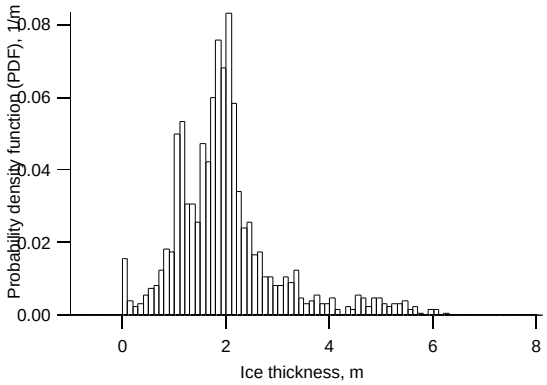

Figure 4: (a) EM and laser derived bird height above the water and ice surface, respectively, and (b) ice thickness profile resulting from subtraction of the latter from the former. (c) Resulting thickness distribution.

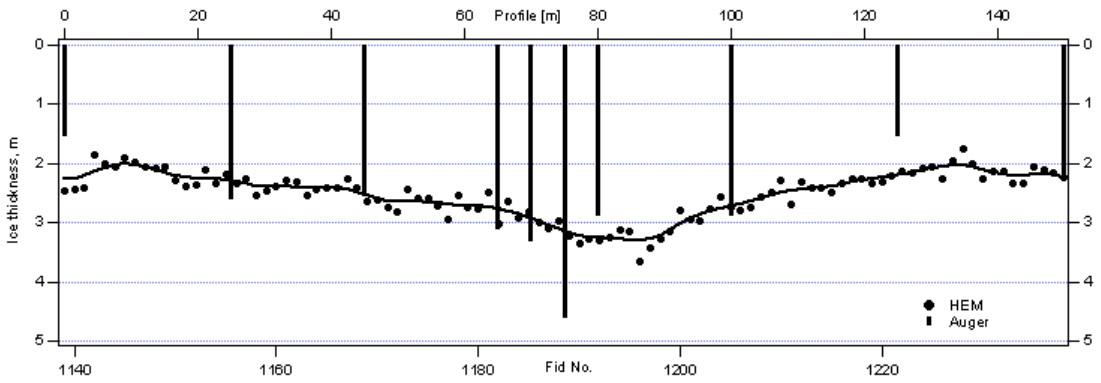

Figure 5: Comparison of helicopter EM thickness estimates with drill-hole measurements obtained over Arctic multiyear ice.

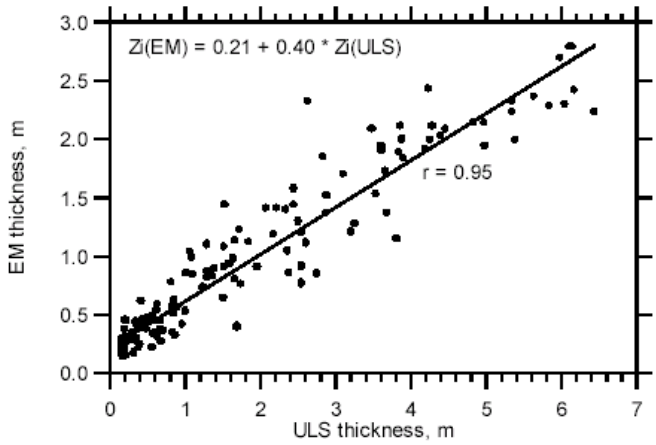

Figure 6: Comparison of coincident EM and ULS ice thickness measurements obtained from the northern Baltic Sea (Haas and Jochmann, 2003).

3. Results and Applications

The main application of EM measurements is the determination of regional thickness distributions and their seasonal, interannual, and decadal variability. Unfortunately, systematic regional thickness monitoring programs are only just initiated, as shown below by the results of our measurements in the Lincoln Sea. Other applications focus on the validation of satellite data and the provision of ground-truth data for algorithm development. For example, we are working on algorithms to estimate surface roughness characteristics from SAR imagery, where the analysis and classification of laser profiler data plays a crucial role. HEM thickness soundings are also the only means for the validation of satellite altimeter data, where the transformation of profiles of freeboard (CryoSat) or surface elevation (ICESat) into ice thickness is the main challenge.

3.1 Ice thickness variability in the Transpolar Drift, 1991-2004

By means of EM sounding, we have irregularly observed the temporal sea ice thickness variability of the Transpolar Drift during August and September since 1991 (Figure 7). The data published by Haas (2004) was updated by HEM flights during cruise ARK 20/2 of RV Polarstern in the summer of 2004. Results showed that modal ice thickness decreased from 2.5 m in 1991 to less than 2 m in 2001, corresponding to a thickness decrease of more than 20% (Haas, 2004). In 2004, the observed modal ice thickness of 2.0 m was only 0.05 m thicker than in 2001 (Figure 7). Thus, there was no further thinning observed between 2001 and 2004. However, we do not know how ice thickness has varied in the meantime.

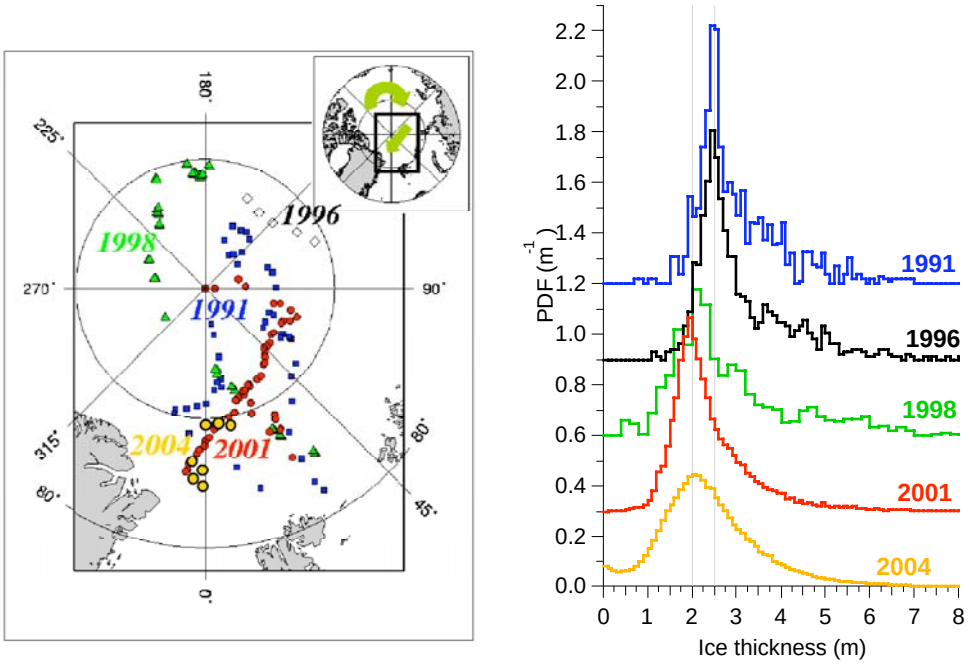

Figure 7: Map of ice thickness measurements performed during summers between 1991 and 2004 in the Transpolar Drift (left). In 2004, all measurements were performed with the EM Bird for the first time. Earlier measurements have been performed by ground-based EM profiling on single floes. Observed ice thickness distributions from the years 1991, '96, '98, 2001 and 2004 had modal thicknesses of 2.5, 2.5, 2.1, 1.95 and 2.0 m respectively (right).

3.2 Ice thickness distribution in the Lincoln Sea, May 2004 and 2005

Funded by the EU GreenICE project, systematic HEM thickness surveying has been initiated in the Lincoln Sea and adjacent Arctic Ocean, north of the Canadian Forces Station Alert on Ellesmere Island at 82.5°N, and between 60 and 70°W. First measurements have been performed in May 2004 and 2005 (Haas et al., 2006). Figure 8 compares the thickness distributions thus obtained. It can be seen that the ice is generally very thick, with modal multiyear ice thicknesses between 3.9 and 4.2 m. However, there are also significant amounts of thinner, likely first year ice with modal thicknesses between 0.9 and 2.2 m. This ice has formed in the recurring Lincoln Polynya. Ice thickness was larger in 2005, with a mean of 5.18 m compared to 4.67 in 2004 (Haas et al., 2006). While the increased modal thickness is partially due to a 0.1 m thicker snow cover in 2005 (with a mode of 0.28 m), ice thickness did also increase by different thermodynamic boundary conditions as well as ice deformation, as can be seen from the longer tail of the 2005 thickness distribution in Figure 8. However, the observed thickness increase is much smaller than would have been expected from the strong southward ice drift towards the coasts of Ellesmere Island and Greenland, as was monitored by drifting GPS buoys (Haas et al., 2006). This is due to ice export through Nares Strait and narrow shear zones along the coasts.

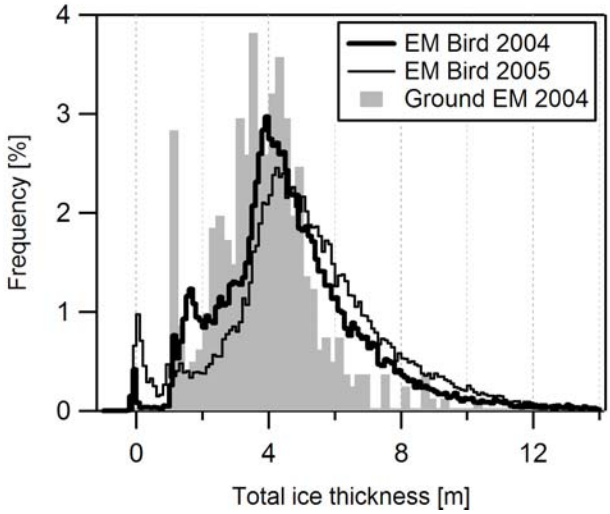

Figure 8: Sea ice thickness distributions of meridional profiles between Alert and 84°N in May 2004 and 2005. The grey-shaded distribution shows the results of the ground-based measurements in 2004 for comparison (Haas et al., 2006).

3.3 Laser profiling of surface roughness and ridge distributions

The laser altimeter included in the EM Bird can be used independently of the EM measurements to obtain information on surface roughness and ridge statistics. Originally, there was no DGPS receiver in the EM Bird to obtain measurements of bird altitude variations, which is necessary to extract the surface roughness profiles (Hvidegaard, xxx; Forsberg et al., this issue). However, the bird altitude variations can also roughly be removed by a combination of different high- and low-pass filters (Hibler, 1972). While this does not allow computation of absolute values of surface elevation, the small scale roughness on scales of some ten meters remains unaffected. Figure 9 shows typical roughness profiles thus obtained, for characteristically different ice types based on the WMO sea ice classification (von Saldern et al., 2006).

We have developed classification algorithms based on the laser data to distinguish between different ice types, and to relate them to ice thickness. A result of a clustering algorithm is shown in Figure 10, where the region around Svalbard is grouped into different degrees of deformation (von Saldern et al., 2006). Unfortunately, there was only weak agreement between roughness and thickness classes. The two thickest ice classes (Thick FY and Old ice) could be discriminated best with the classification technique, and it was also possible to distinguish these thicker classes from the three thinner classes. The three thinner ice classes could not be separated.

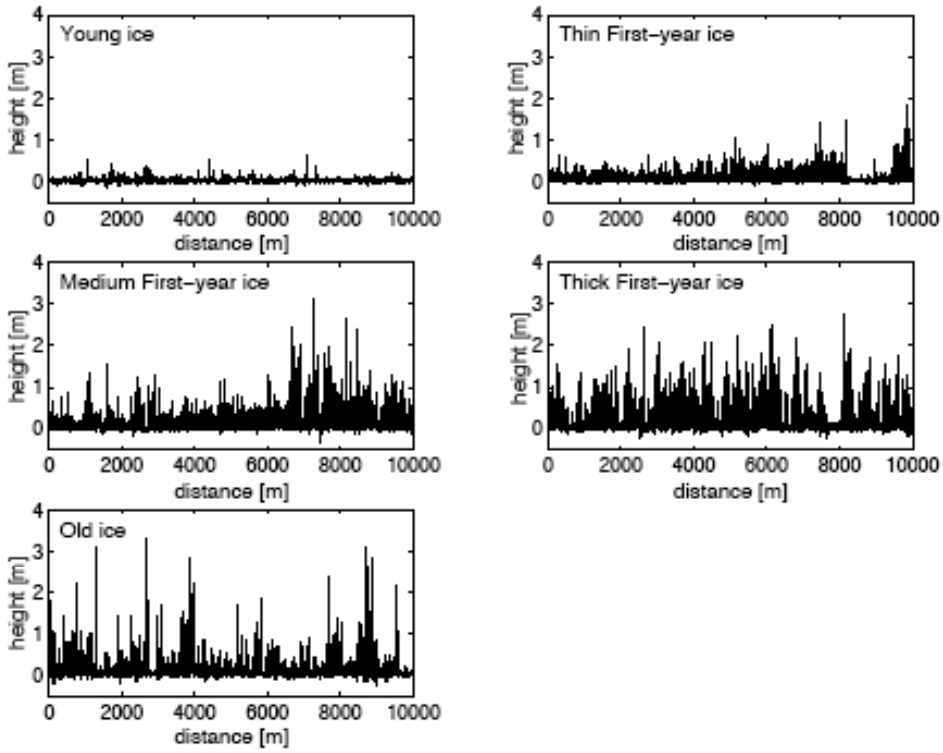

Figure 9: Surface roughness profiles of different ice types, which have been used to develop algorithms for their objective classification (von Saldern et al., 2006).

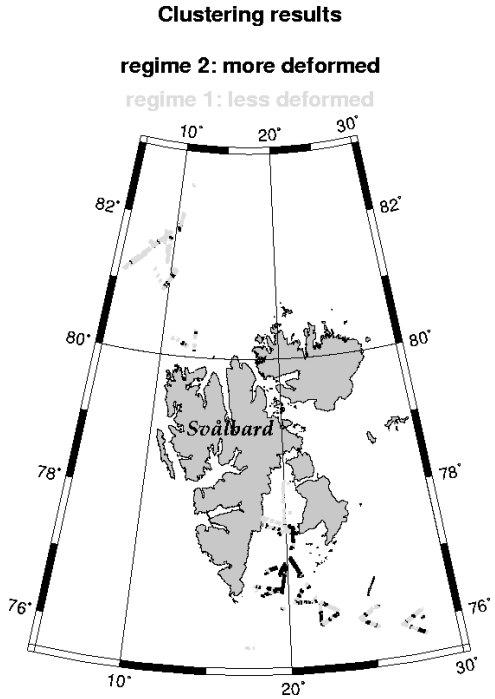

Figure 10: Geographical distribution of two roughness regimes around Svalbard in March and April 2003, in Storfjord and the Barents Sea, and in Fram Strait (von Saldern et al., 2006).

The surface roughness profiles can also be used to identify pressure ridges. This is routinely done with all EM Bird data, as it provides additional information on the amount and thickness of deformed ice, which is underestimated from the EM thickness data alone. Figure 11 summarizes the results thus obtained during GreenICE and SITHOS HEM campaigns to the Lincoln Sea, Fram Strait, Barents Sea, and to the Baltic Sea. Sail height distributions possess the well-known exponential decline towards higher sails (Fig. 11, left panel). The distribution changes its steepness from the thin first year ice of the Baltic to the heavily deformed multiyear ice in the Lincoln Sea north of Greenland and the Canadian Archipelago. Barents Sea and Fram Strait feature ice regimes that are of intermediate deformation state, representing Arctic thick first-year and thin multiyear ice. Differences in the distributions of ridge density (Fig. 11, right panel) closely correspond to the characteristics of the respective ridge height distributions. Ridge density is the number of ridges per kilometre and is calculated from the sail spacing of 5 km long legs. The thin and thick first-year ice of the Baltic and Barents Seas shows rather small modal ridge densities of only 1 km^{-1}, for a cut-off height of 0.8 m. In Fram Strait and the Lincoln Sea larger ridges are more frequent, up to 16 km^{-1}. It is interesting to note that also in the Barents Sea are second, smaller mode occurs at 20 km^{-1}. This mode originated from heavily deformed second-year ice in the entrance of Storfjord, which was advected into the Barents Sea by the East Spitzbergen Current in March 2003.

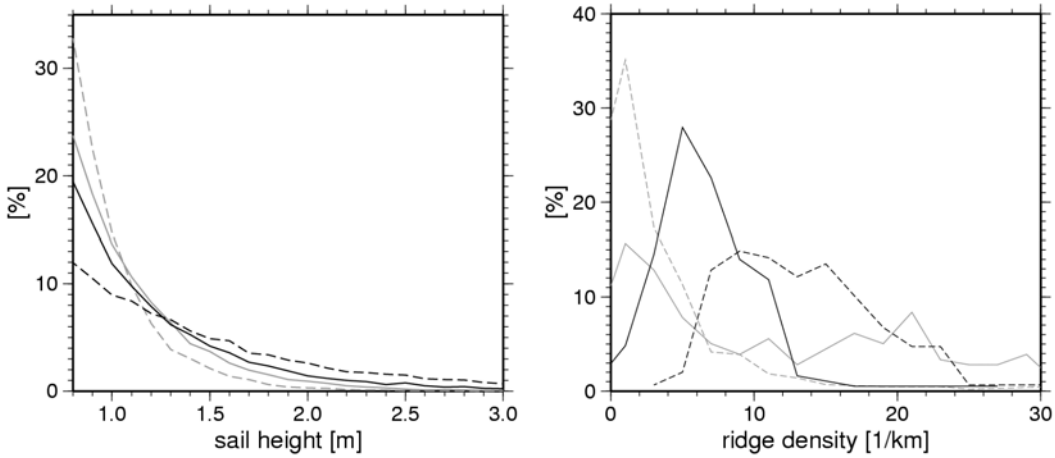

Figure 11: Frequency distributions of sail height (left panel) and ridge density (right panel) in Fram Strait (solid black), in the Lincoln Sea (dashed black), in the Barents Sea (solid grey), and in the Baltic Sea (dashed light grey) derived from HEM laser profiles. Ridge statistics have been computed for a cut-off height of 0.8 m.

3.4 Snow thickness measurements using laser altimetry, DGPS, and total thickness estimates

Since 2004, a DGPS receiver is included in our EM Bird for the accurate determination of surface elevation from laser and DGPS data. With the DGPS data, the bird altitude variations can be accurately removed from the laser measurements. Therefore, the EM Bird now acquires coincident profiles of ice thickness and surface elevation, allowing to prove the concepts of ICESat and CryoSat ice thickness retrievals.

Key to accurate thickness retrievals from satellite altimetry is the transformation of surface elevation to ice thickness by multiplying the former with a factor R, which is a

function of snow depth and the densities of snow and ice (Wadhams et al., 1992). While these are generally not known with sufficient accuracy, the situation is even more complicated if different ice and snow thickness classes are present. Figure 12 shows an example from the Lincoln Sea, where thick MY ice and thinner FY ice were present in May 2005. The histogram of surface elevation can be transformed into a thickness distribution matching the EM-derived data, if varying R-factors are assumed for different surface elevations.
In the example of Figure 12, R-factors were computed from the modes of the thickness and surface-elevation distributions as given in the Figure. They were R = 6.3 and R = 5.74 for first-year and multiyear ice, respectively.
From the varying R-factors, different snow thicknesses can be calculated, if isostatic equilibrium and certain values for the densities of seawater, ice, and snow are assumed. In the example of Figure 12, modal snow thicknesses of 0.16 and 0.44 m result for the first-year and multiyear ice, with water, ice, and snow densities of 1024, 915, and 300 kg m^{-3}, respectively. These results are in good agreement with direct measurements on the ground (Haas et al., 2006). However, our results show that R varies widely between values of 5 and 8, and that functions of R versus surface elevation have to be tuned for any different ice type.

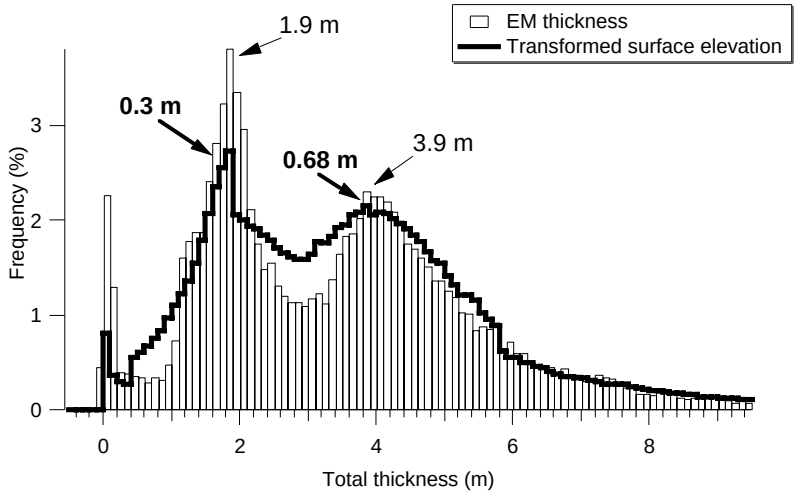

Figure 12: Comparison of ice thickness distributions in the Lincoln Sea in May 2005, derived from EM thickness sounding and from coincident laser/DGPS measurements of surface elevation. The distribution of surface elevations was transformed into an ice thickness distribution using R-factors derived from matching local modes of both distributions, given by the numbers (bold: surface elevation; plain: ice thickness).

4. Conclusions and outlook

EM thickness sounding is a powerful tool for accurate thickness measurements. The accuracy of retrievals of level ice thickness is better than ±0.1 m. However, over deformed ice, the maximum thickness of ridge keels could be underestimated by as much as 50 or 60%. Nevertheless do the measurements provide information about the amount of deformed ice in the survey region (Fig. 11), and ridge thicknesses can be distinguished relatively, as shown by our EM/ULS comparison (Fig. 6) and by the surveys in the Lincoln Sea in 2004 and 2005 (Fig. 8). The method is therefore well understood and robust, and can now be applied for more systematic measurements,

like e.g. for the thickness monitoring program we have just initiated in the Lincoln Sea and adjacent Arctic Ocean.
To better understand and possibly correct for the underestimation of deformed ice thickness, 2- and 3D- EM modelling studies are required. These need to take into account not only the 3D structure of the ridges, but also the high ridge porosity, comprising of large seawater-filled, interconnected voids and large ice blocks. The connectivity of the voids leads to channelling effects of the eddy currents, which may prevent any deeper penetration of the EM fields. However, different EM channels will have variable sensitivity to these conditions, and therefore multi-channel inversion procedures could improve the thickness retrievals over deformed ice.
Ultimately, more coincident ULS and EM measurements under Arctic conditions should be performed to obtain profiles of ULS daft and EM ice thickness for direct comparison. Unfortunately, an attempt during RV Polarstern cruise ARK 20 in 2004 failed due to bad weather, when RV Polarstern and British HMS J.C. Ross met with the intention to perform joint measurements with the UK Autosub. Therefore, any other opportunity would be highly appreciated.
Although HEM thickness surveying is a big step forward for systematic measurements, limited range of helicopter operations of 300 to 400 km still poses a problem for larger scale studies. Therefore, we strongly encourage international cooperation, e.g. in the usage and joint deployment of fuel depots and other infrastructure in the Arctic to extend operation range. For example, during IPY 2007 and 2008 we plan to survey across the whole Arctic Ocean, jointly with logistical support from US, Danish, and Russian colleagues. We do also loan our birds to other groups who might have access to ship cruises and helicopter time. The operation range can also be extended by usage of fixed wing aircrafts. For example, we are currently developing an EM system for our DO228 research aircraft at Alfred Wegener Institute. Similarly, jointly with French colleagues we plan to cross the Arctic Ocean with a Zeppelin airship in 2007. However, any survey based on EM sounding has to be performed at low system altitudes of < 30 m, which poses another limitation on the method.
EM surveys yield the total sea ice thickness, i.e. the sum of ice and snow thickness. Snow thickness is another important but extremely difficult to measure climate variable. Our new results using EM thickness surveying combined with laser profiling and DGPS flight-altitude measurements point to en exciting new possibility to retrieve both snow and ice thickness from a single bird flight. We will perform an extensive validation study of this technique during September 2006 in the Weddell Sea.

Acknowledgements
We are most gratefully to E. Augstein and H. Miller for initiating this work, and for AWI funding. Geophysical and technical contributions by K.P. Sengpiel, J. Lohbach, and staff of Aerodata and Optimare are greatly acknowledged. Numerous students improved the data processing procedures. All developments benefited from extensive tests flights with Helicopter Service Wasserthal and Helitransair.

References
Forsberg et al., 2006: xxx this issue.
Haas, C., S. Gerland, H. Eicken, and H. Miller, 1997: Comparison of sea-ice thickness measurements under summer and winter conditions in the Arctic using a small electromagnetic induction device. *Geophysics* 62, 749-757.

Haas, C., 1998: Evaluation of ship-based electromagnetic-inductive thickness measurements of summer sea-ice in the Bellingshausen and Amundsen Seas, Antarctica. *Cold Regions Science and Technology* 27, 1-16.

Haas, C., K.-H. Rupp, and A. Uuskallio, 1999: Comparison of along track EM ice thickness profiles with ship performance data. *Proceedings of the 15th International Conference on Port and Ocean Engineering under Arctic Conditions, Espoo, Finland, 1999, Helsinki Univ Techn, Ship Lab*, 1, 343-353.

Haas, C., and H. Eicken, 2001: Interannual variability of summer sea ice thickness in the siberian and central Arctic under different atmospheric circulation regimes. *Journal of Geophysical Research* 106 (C3), 4449-4462.

Haas, C., and P. Jochmann, 2003: Continuous EM and ULS thickness profiling in support of ice force measurements*. Proceedings of the 17th International Conference on Port and Ocean Engineering under Arctic Conditions, POAC ´03, Trondheim, Norway, Department of Civil and Transport Engineering, Norwegian University of Science and Technology NTNU, Trondheim, Norway*,2, 849-856.

Haas, C., 2004: Airborne EM sea-ice thickness profiling over brackish Baltic sea water. *Proceedings of the 17th international IAHR symposium on ice, June 21-25, 2004, St. Petersburg, Russia, All-Russian Research Institute of Hydraulic Engineering (VNIIG), Saint Petersburg, Russia,* 2, 12-17.

Haas, C., S. Hendricks and M. Doble, 2006: Comparison of the sea ice thickness distribution in the Lincoln Sea and adjacent Arctic Ocean in 2004 and 2005. *Annals of Glaciology* 44, in press

Hibler, W.D. III, 1972: Removal of aircraft altitude variation from laser profiles of the Arctic ice pack. *J. Geoph. Res.* 77(36), 7190-7195.

Hvidegaard S. M., and R. Forsberg, 2002: Sea-ice thickness from airborne laser altimetry over the Arctic Ocean north of Greenland. *Geophys. Res. Lett.,* 29 (20), 1952, doi:10.1029/2001GL014474.

Kovacs, A., N.C Valleau, and J.S. Holladay, 1987: Airborne electromagnetic sounding of sea ice thickness and sub-ice bathymetry. *Cold Regions Science and Technology* 14, 289-311.

Kovacs, A., and J.S. Holladay, 1990: Sea-ice thickness measurements using a small airborne electromagnetic sounding system. *Geophysics* 55, 1327-1337.

Kovacs, A., J.S. Holladay, and C.J. Bergeron, 1995: The footprint/altitude ratio for helicopter electromagnetic sounding of sea-ice thickness: Comparison of theoretical and field estimates. *Geophysics* 60, 374-380.

Multala, J., H. Hautaniemi, M. Oksama, M. Leppäranta, J. Haapala, A. Herlevi, K. Riska, and M. Lensu, 1996: An airborne electromagnetic system on a fixed wing aircraft for sea ice thickness mapping. *Cold Reg. Sci. Techn* 24, 355-373.

Pfaffling, A., C. Haas, and J. Reid, 2006: Key characteristics of helicopter electromagnetic sea ice thickness mapping: Resolution, accuracy, and footprint. EU report series, Ice tickness workshop in Copenhagen, this issue.

Prinsenberg, S.J., and J.S. Holladay, 1993: Using air-borne electromagnetic ice thickness sensor to validate remotely sensed marginal ice zone properties. *Port and ocean engineering under arctic* conditions *(POAC 93), HSVA (Ed)*, Vol. 2, 936-948.

Reid, J., A. Pfaffling, and J. Vrbancich, 2006: Airborne electromagnetic footprints in one-dimensional earths. *Geophysics* 71(2). G63-G72, doi: 10.1190/1.2187756.

Saldern, C., C. Haas, and W. Dierking, 2006: Parameterisation of Arctic sea ice surface roughness for application in ice type classification. *Annals of glaciology* 44, in press.

Wadhams, P., W.B. Tucker III, W.B. Krabill, R.N. Swift, J.C. Comiso, and N.R. Davis, 1992: Relationship between sea ice freeboard and draft in the Arctic Basin, and implications for ice thickness monitoring. *J. Geoph. Res.* 97(C12), 20,325-20,334.

Ward, S. H., and G.W. Hohmann, 1988: Electromagnetic theory for geophysical applications. *Electromagnetic methods in applied geophysics-theory, volume 1*, SEG Monograph, (M.N. Nabighian, Ed.), Vol. 3, 131-313.